

# NanoSQUIDs With Proximity Effect Nanobridge Josephson Junctions for Future Applications in Electron Microscopy

Michael I. Faley , Joseph Vimal Vas , Penghan Lu , and Rafal Dunin-Borkowski 

**Abstract**—Nanoscale superconducting quantum interference devices (nanoSQUIDs) with nanobridge Josephson junctions (nJJs) were prepared on SiN membranes for experiments with transmission electron microscope (TEM) at temperatures below 10 K. As thin-film materials for the nanobridges, metals Ti and Nb were combined into 3-layer heterostructures for adjusting superconducting parameters of the nJJs through the proximity effect. This allowed to reduce spread of parameters in ultrathin superconducting films and to adjust operating temperature of nJJs to the optimum operating temperature of the commercial TEM sample holders cooled using liquid helium. Electron beam lithography and high selectivity reactive ion etching with pure SF<sub>6</sub> gas were used to pattern nJJs with down to 10 nm width that is comparable to coherence length in thin films of Nb. Measurements revealed non-hysteretic  $I(V)$  characteristics of the nJJs and nanoSQUIDs. The paper is mainly devoted to the development of nanoSQUIDs for possible applications in TEM. Towards realization of hybrid superconductor-ferromagnetic nanostructures for further experiments in TEM, Permalloy triangles with spatial resolution down to  $\sim 100$  nm were prepared on similar SiN membranes and studied by Lorentz TEM method. These technologies are promising for the fabrication of superconducting electronics based on nJJs for operation inside a TEM.

**Index Terms**—Electron beam lithography, Josephson devices, proximity effect, sputtering, SQUIDs, transmission electron microscope.

## I. INTRODUCTION

THE miniaturization of superconducting circuits follows, with some delay, the trend toward miniaturization of semiconductor electronics. Reducing the size of superconducting components such as Josephson junctions, inductors, current leads, etc., nonlinearly changes their properties due to spatial variation in the macroscopic wave function of phase-correlated Cooper pairs propagating over relatively large distances of the order of the coherence length and the London penetration depth in superconductors. This significantly complicates the theoretical description and requires empirical optimization of individual components in dense superconducting circuits taking into account their correlation with spatial variation of the

crystallographic and chemical properties due to granularity of the films. In this case, transmission electron microscope (TEM) is capable of analyzing physical properties at the nanometer scale: not only microstructural studies at room temperature, such as crystal structure, stoichiometry, thin film growth, defect and grain formation, but also their functionality at low temperatures [1], [2]. Using commercially available sample holders [3], [4], routine cooling of samples down to  $\sim 5$  K in TEM is now possible that allows direct observation of correlation between microstructure and functionality of superconducting devices.

Imaging flux vortices in type II superconductors does not require galvanic contacts to the sample and was demonstrated with a commercial TEM: see [5] and references therein. For operating superconducting circuits galvanic contacts are essential and can be realized using TEM sample holders of condenZero AG [3]. Also Gatan [4] provide liquid helium cooled TEM holders with electrical feedthroughs that can be used to make galvanic contacts to the sample.

The reduction in the size of Josephson junctions from the first  $0.025 \times 0.065$  cm<sup>2</sup> [6] to the modern 10 nm  $\times$  10 nm (see [7] and references therein) is a clear demonstration of technological progress in the history of superconducting electronics. Nanobridge Josephson junctions (nJJs) can theoretically observe an almost ideal Josephson behavior [8]. NanoSQUIDs with nJJs and similar superconducting components seems to be the most suitable devices for the first tests of their operation in TEM because of their small size and thickness they must fit within the field of view of a holographic TEM of a few microns in size and be transparent to the electron beam. Strong temperature dependence of critical current  $I_c$  of Dayem-type nJJs and nanoSQUIDs with such nJJs limits their operation temperature range to the  $(T_c - T)/T_c < 0.2$  vicinity of superconducting transition temperature  $T_c$ . This demands fine tuning of  $T_c$  for the superconducting films involved in the nJJs and nanoSQUIDs. The optimization of  $T_c$  can be performed by using proximity effect with normal conducting films of different thicknesses [9]. The superconducting components can be combined with single layer nanostructures of ferromagnetic and other quantum materials for realization of effective spintronic devices.

In the present work, we describe preparation of a nanoSQUID with nJJs patterned from a 3-layer heterostructure film with engineered  $T_c$  using proximity effect, placed on a SiN membrane and studied using TEM with spatial resolution down to

Received 25 September 2024; revised 12 November 2024; accepted 15 November 2024. Date of publication 19 November 2024; date of current version 6 December 2024. (Corresponding author: M. I. Faley.)

The authors are with ER-C-1, Forschungszentrum Jülich GmbH, 52428 Jülich, Germany (e-mail: m.faley@fz-juelich.de).

Color versions of one or more figures in this article are available at <https://doi.org/10.1109/TASC.2024.3502572>.

Digital Object Identifier 10.1109/TASC.2024.3502572

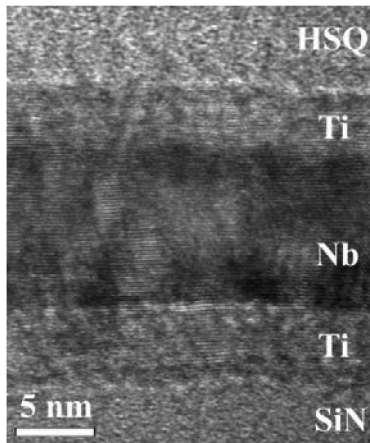


Fig. 1. High resolution TEM image of a HSQ resist-covered heterostructure consisting of two 4 nm thick Ti films with an 8 nm thick Nb film in between, fabricated on a SiN buffer layer on a Si substrate.

atomic level. The paper is mainly devoted to the development of nanoSQUIDs for possible applications in TEM. Towards realization of hybrid superconductor-ferromagnetic nanostructures for further experiments in TEM like presented in [10], Permalloy (Py) triangles were placed on similar SiN membranes and their in-plane magnetization was studied with spatial resolution down to few nanometers using Lorenz TEM (LTEM).

## II. EXPERIMENTAL

The SiN-buffered Si substrates were cleaned in acetone, propanol, and deionized water before placing them in a home-built sputtering machine, which was evacuated to a base pressure of  $< 4 \times 10^{-8}$  mbar using oil-free pumps. Before deposition, the chamber was outgassed under deposition conditions during presputtering onto the closed shutter for more than 10 min.

During deposition, the substrates were placed freely on a heater at 100°C in argon with a purity of 99.9999% at 1 Pa pressure. Ti and Nb films were deposited at a rate of  $\sim 15$  nm/min from 50 mm diameter 99.95% pure Ti and Nb targets using pulsed reactive DC magnetron sputtering. Thin-film Ti(4 nm)-Nb(8 nm)-Ti(4 nm) heterostructures were prepared on SiN-buffered Si substrates and spin-coated by 35 nm thick HSQ resist XR-1541-002. The corresponding high resolution TEM image was obtained using FEI Titan 80–300 microscope and shown in Fig. 1. A columnar growth of the grains was observed and they spread throughout the entire thickness of the heterostructure. The Ti- and Nb-layers are polycrystalline with average in-plane size of grains  $\sim 5$  nm and [110]-axis oriented normal to the substrate surface with the interplanar spacing of  $\sim 0.24$  nm [11]. The in-plane *a*- and *b*-axis lattice constants of Ti and Nb are about  $\sim 0.3$  nm [12], [13].

The lowest 4 nm thick Ti layer served as a buffer layer for the subsequent Nb film and improved its  $T_c$  and critical current. The uppermost 4 nm thick Ti layer in the Ti-Nb-Ti heterostructure served for the fine setting of  $T_c$  using proximity effect, for a better adhesion of HSQ resist and for the protection of the 8 nm thick Nb layer from corrosion and oxidation during

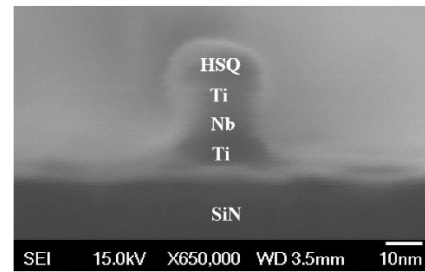


Fig. 2. Cross-sectional SEM image of a HSQ resist-covered heterostructure consisting of two 4 nm thick Ti films with an 8 nm thick Nb film in between, fabricated on a SiN buffer layer on a Si substrate.

patterning by EBL. These particular thicknesses are also result of optimization of  $T_c$  for the trilayer film that should be about 5.5 K for optimal operation of nJJs at 5 K stabilized temperature in TEM holder. Increasing the thickness of Ti layers decreases  $T_c$ , while increasing the thickness of Nb layer increases  $T_c$ . Too thin Nb layer widens the superconducting transition and increases device noise.

HSQ resist was patterned with spatial resolution down to  $\sim 10$  nm using exposure by e-beam at acceleration voltage 100 kV and dose 3 mC/cm<sup>2</sup> and highly selective reactive ion etching (RIE) in pure SF<sub>6</sub> gas. The RIE process provides  $\sim 3$  times faster etch rates for Ti and Nb in comparison to SiN and the HSQ resist. The 16 nm thick Ti-Nb-Ti heterostructures have an undercut of  $< 5$  nm, which is  $\sim 10$  times smaller than the undercut observed in the preparation of pure 100 nm thick TiN nJJs [14]. The smaller undercut resulted in improved reproducibility of the nJJs and a spatial resolution of the superconducting nanostructures that approached the spatial resolution of the HSQ resist mask.

Fig. 2 shows a cross-sectional SEM image of a HSQ resist-covered heterostructure consisting of two 4 nm thick Ti films with an 8 nm thick Nb film in between, fabricated on a SiN buffer layer. After RIE no re-sputtered material (fences) was observed. Instead, a few nanometer-wide undercut of  $< 5$  nm made the structures effectively narrower than in HSQ mask.

We used 200  $\mu\text{m}$  thick Si substrates that were buffered on both sides by 100 nm thick low-stress SiN films using low-pressure chemical vapor deposition (LPCVD). The superconducting and ferromagnetic films were deposited and nanostructured under standard conditions on bulk substrates, followed by wet chemical etching of the Si substrate in 20% KOH from the back side of the substrate to the back side of the SiN buffer layer using homemade holders. Simultaneously with a 50  $\mu\text{m} \times 50$   $\mu\text{m}$  window with the membrane, the outside of the TEM grid with standard diameter 3 mm was etched. The etch rate of Si in the KOH solution at 60 °C was approximately 9 nm/h.

## III. RESULTS

The thin-film Ti(4 nm)-Nb(8 nm)-Ti(4 nm) heterostructures fabricated on a Si substrate covered with a low-stress LPCVD SiN buffer layer have  $T_c \cong 5.5$  K (see Fig. 3) that was empirically optimized for optimal non-hysteretic operation of nJJs and nanoSQUIDs based on these multilayer films.

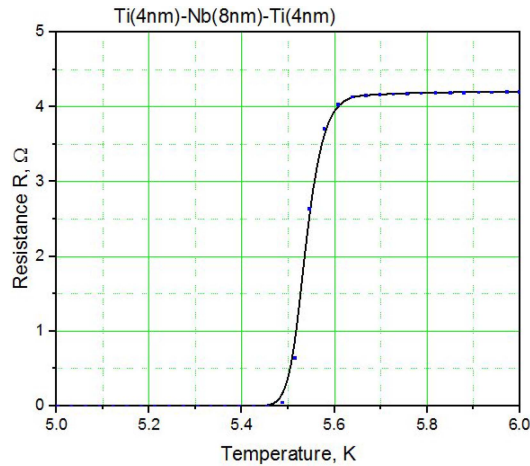


Fig. 3.  $R(T)$ -dependence in the vicinity of superconducting transition at 5.5 K of a heterostructure consisting of two 4 nm thick Ti films with an 8 nm thick Nb film in between, fabricated on a Si substrate covered with a low-stress SiN buffer layer.

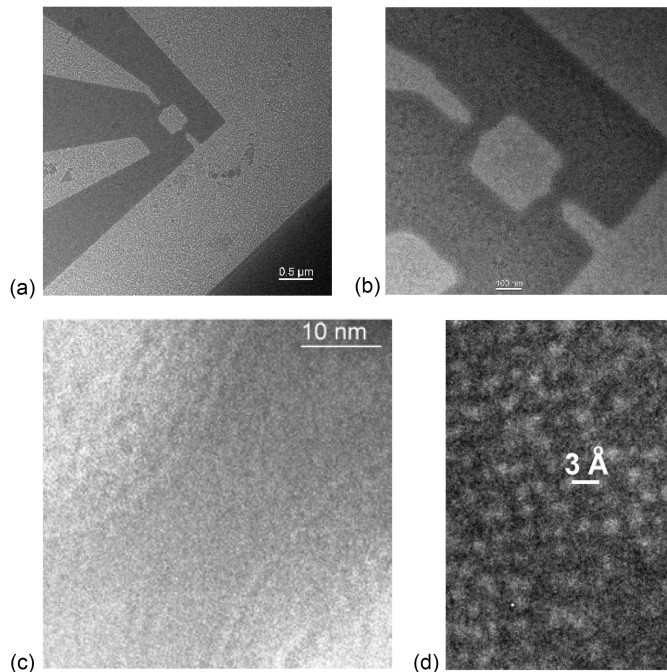


Fig. 4. Plan-view TEM images of a nanoSQUID fabricated on a SiN membrane: (a) low-magnification TEM image showing position of nanoSQUID relative to the edge of membrane; (b) a higher magnification TEM image showing microcrystalline structure of the membrane and a polycrystalline structure of the Ti-Nb-Ti heterostructure film; (c) a higher magnification TEM image of one of the nJJs demonstrating width of the nJJ and HSQ resist; and (d) high resolution TEM image of Ti-Nb-Ti heterostructure in nJJ in nanoSQUID showing the  $\sim 0.3$  nm interatomic distance corresponding to the lattice constant of Ti and Nb.

NanoSQUIDS were fabricated on a 100 nm thick, low-strain SiN membrane near one of the membrane edges (Fig. 4(a)). A microcrystalline structure of the membrane and a polycrystalline structure of the Ti-Nb-Ti heterostructure film are observed in the plan-view TEM image (Fig. 4(b)). A higher magnification TEM image of one of the nJJs demonstrated width of the nJJ under

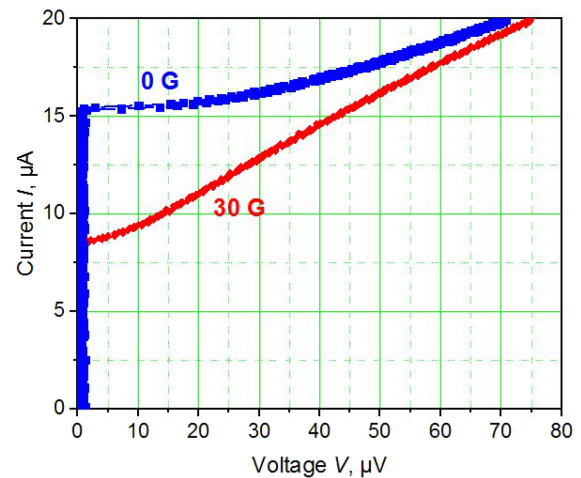


Fig. 5.  $I(V)$  characteristics of a nanoSQUID recorded in 0 G (blue) and 30 G (red) magnetic fields at 4.2 K. The voltage swings for the modulation in magnetic field are  $>40$   $\mu\text{V}$  at a bias current of 16  $\mu\text{A}$ .

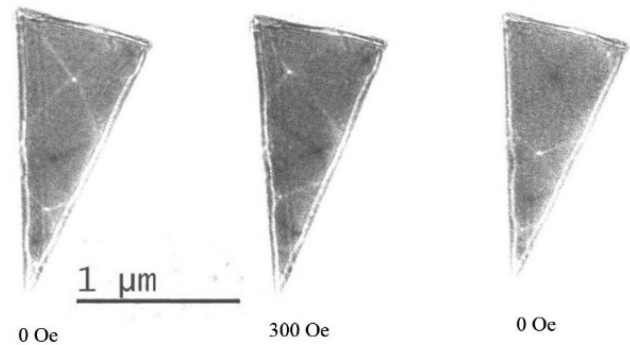


Fig. 6. LTEM images of a Py triangle in different magnetic fields. A successfully performed repolarization of the magnetization states in this nanostructure is demonstrated.

mask of HSQ resist (Fig. 4(c)). A high resolution TEM image of Ti-Nb-Ti heterostructure in nJJ in nanoSQUID (Fig. 4(d)) showed the  $\sim 0.3$  nm interatomic spacing that corresponds approximately to the lattice constant in  $ab$ -planes of Ti and Nb [12], [13].

$I(V)$  characteristics of nanoSQUIDS observed critical current  $\sim 16$   $\mu\text{A}$  and a strong periodic dependence on magnetic field with a period of  $\sim 60$  G (Fig. 5). At bias current  $> \sim 30$   $\mu\text{A}$  characteristics becomes unstable observed thermal hysteresis (not shown in Fig. 5) due to overheating and reduced heat removal of nJJs on membrane: the heat is originated from the Joule heating and partially heating from Josephson radiation. The corresponding critical current and the amplitude of the thermal hysteresis depend exclusively on the heat dissipation and are independent of the magnetic field [15].

Triangles from 50 nm thick Py ( $\sim 80\%$  Ni and  $\sim 20\%$  Fe) films were also prepared on SiN membranes (Fig. 6) for future combination with the superconducting circuits. Like Ti and Nb, Py is also compatible with CMOS applications [16], making it a preferred choice for ferromagnetic materials in electronics. We deposited thin films of Py at room temperature using dc magnetron sputtering from a single target in a pure Ar atmosphere at

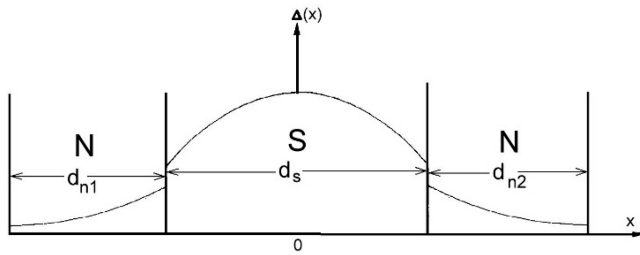


Fig. 7. Variation of the pair potential  $\Delta(x)$  across a NSN triple layer.

a pressure of  $\sim 1$  Pa. A lift-off technique was used for patterning of Py films on membranes and provided spatial resolution better than 100 nm [2].

The Py triangles were studied by LTEM [17] using FEI Titan G2 60-300 HOLO microscope. Fig. 6 shows LTEM images of a Py triangle in different magnetic fields. The white and dark points and lines indicate the directions of in-plane magnetization inside the Py triangle and demonstrate the successfully performed repolarization of the magnetization state in this nanostructure.

#### IV. DISCUSSION

The Ti-Nb-Ti heterostructure was chosen for the present work due to its relatively large coherence length at 5 K operating temperature of  $\xi(5\text{ K}) \sim 27$  nm, which is comparable to the routinely achieved dimensions  $\sim 10$  nm of the nJJs (Fig. 2). This ensures an almost ideal Josephson behavior of the nJJs [8].

We have successfully used proximity effect to adjust  $T_c$  of the Ti-Nb-Ti heterostructure. Schematically the suppression of the pair potential and, correspondingly,  $T_c$  in the heterostructure is demonstrated in Fig. 7. The related equations can be found in the reference [9] where the estimates were done for a bilayer that can be interpreted as a half of the investigated 3-layer heterostructure. The suppression of  $T_c$  in the superconducting layer is much stronger and more uniform in the 3-layer heterostructure than in the two-layer one. Similar considerations can be taken into account for adjusting  $T_c$  of TiN-NbN-TiN heterostructures [2].

Operation of nanoSQUID on membrane is complicated by reduced heat removal that is leading to increased thermal hysteresis. Placing the nanoSQUID outside the SiN window or in close proximity to the corner of the cantilever [15] largely solves this problem.

We have fabricated nanoSQUIDs and Py triangles on SiN membranes and studied them separately. The period of voltage modulation of nanoSQUID  $\sim 60$  G and magnetic field required for switching of Py triangle  $\sim 300$  G were measured. These comparable values are convenient for the experiments including both structures. High currents flowing without energy dissipation in superconducting circuits or high frequency Josephson oscillations in nJJs can be used for exciting spin-resonances in ferromagnetic nanostructures. The corresponding in-plane magnetic fields could be observed by TEM while out-of-plane stray fields could be observed by a nanoSQUID. To place Py

nanostructures near nanoSQUIDs in future experiments, one could use the nanomanipulator of a focused ion beam machine in the case of a cantilever-based nanoSQUID, or fabricate both structures on a single bulk substrate before performing KOH etching in the case of a membrane-based nanoSQUID.

#### V. CONCLUSION

For the first time, we have fabricated nanoSQUIDs with nJJs on SiN membranes that are intended for low temperature experiments in TEM. The operating temperature of Nb nJJs was adjusted to the optimal operating temperature of 5 K in the liquid helium-cooled commercial TEM sample holder by exploiting the proximity effect in 3-layer heterostructure Ti-Nb-Ti. Electron beam lithography and high selectivity reactive ion etching with pure  $\text{SF}_6$  gas were used to pattern nJJs with down to  $\sim 10$  nm width that is comparable to coherence length in thin films of Nb. The paper focuses on the development of nanoSQUIDs for possible future applications in TEM. Towards realization of hybrid superconductor-ferromagnetic nanostructures for experiments in TEM, Py triangles with spatial resolution down to  $\sim 100$  nm were prepared on SiN membranes and studied by LTEM method. These technologies are promising for the fabrication and study of superconducting circuits based on nJJs for operation inside a TEM.

#### ACKNOWLEDGMENT

The authors gratefully acknowledge the opportunity to perform parts of the work at ER-C-1, HNF, JCNS-2, and PGI-7 in Forschungszentrum Jülich GmbH. The authors also thank R. Borowski, L. Kibkalo, L. Risters, H. Stumpf, M. Nonn, S. Trelenkamp, F. Lentz, S. Neduev, E. Neumann, O. Petravic, S. Nandi, B. Schmitz, and G. Potemkin for technical assistance.

#### REFERENCES

- [1] Y. Li, W. Huang, Y. Li, W. Chiu, and Y. Cui, "Opportunities for cryogenic electron microscopy in materials science and nanoscience," *ACS Nano*, vol. 14, no. 8, pp. 9263–9276, 2020, doi: [10.1021/acsnano.0c05020](https://doi.org/10.1021/acsnano.0c05020).
- [2] M. I. Faley, J. Williams, P. Lu, and R. E. Dunin-Borkowski, "TiN-Nb-TiN and permalloy nanostructures for applications in transmission electron microscopy," *Electronics*, vol. 12, no. 9, 2023, Art. no. 2144, doi: [10.3390/electronics12092144](https://doi.org/10.3390/electronics12092144).
- [3] condenZero AG, Accessed: Sep. 21, 2024. [Online]. Available: <https://condenzero.com/>
- [4] Gatan, Accessed: Nov. 10, 2024. [Online]. Available: <https://www.gatan.com/products/tem-specimen-holders/cooling-situ-holders>
- [5] J. C. Loudon and P. A. Midgley, "Imaging flux vortices in type II superconductors with a commercial transmission electron microscope," *Ultramicroscopy*, vol. 109, pp. 700–729, 2009, doi: [10.1016/j.ultramic.2009.01.008](https://doi.org/10.1016/j.ultramic.2009.01.008).
- [6] P. W. Anderson and J. M. Rowell, "Probable observation of the Josephson superconducting tunneling effect," *Phys. Rev. Lett.*, vol. 10, pp. 230–232, 1963, doi: [10.1103/PhysRevLett.10.230](https://doi.org/10.1103/PhysRevLett.10.230).
- [7] R. Rodrigo, M. I. Faley, and R. E. Dunin-Borkowski, "NanoSQUIDs based on Nb nanobridges," in *Proc. J. Phys., Conf. Ser.*, 2020, Art. no. 012011, doi: [10.1088/1742-6596/1559/1/012011](https://doi.org/10.1088/1742-6596/1559/1/012011).
- [8] K. Likharev, "Superconducting weak links," *Rev. Modern Phys.*, vol. 51, no. 1, pp. 101–159, 1979, doi: [10.1103/RevModPhys.51.101](https://doi.org/10.1103/RevModPhys.51.101).
- [9] J. M. Martinis, G. C. Hilton, K. D. Irwin, and D. A. Wollman, "Calculation of  $T_c$  in a normal-superconductor bilayer using the microscopic-based usadel theory," *Nucl. Instrum. Methods Phys. Res. A*, vol. 444, pp. 23–27, 2000, doi: [10.1016/S0168-9002\(99\)01320-0](https://doi.org/10.1016/S0168-9002(99)01320-0).

- [10] S. Gupta, R. Medwal, D. Kodama, K. Kondou, Y. Otani, and Y. Fukuma, "Important role of magnetization precession angle measurement in inverse spin Hall effect induced by spin pumping," *Appl. Phys. Lett.*, vol. 110, 2017, Art. no. 022404, doi: [10.1063/1.4973704](https://doi.org/10.1063/1.4973704).
- [11] X. Li, W. Cao, X. Tao, L. Ren, L. Zhou, and G. Xu, "Structural and nanomechanical characterization of niobium films deposited by DC magnetron sputtering," *Appl. Phys. A*, vol. 122, 2016, Art. no. 505, doi: [10.1007/s00339-016-9990-1](https://doi.org/10.1007/s00339-016-9990-1).
- [12] R. M. Wood, "The lattice constants of high purity alpha titanium," *Proc. Phys. Soc.*, vol. 80, no. 3, pp. 783–786, Sep. 1962, doi: [10.1088/0370-1328/80/3/323](https://doi.org/10.1088/0370-1328/80/3/323).
- [13] R. Roberge, "Lattice parameter of niobium between 4.2 and 300 K," *J. Less-Common Met.*, vol. 40, no. 1, pp. 161–164, doi: [10.1016/0022-5088\(75\)90193-9](https://doi.org/10.1016/0022-5088(75)90193-9).
- [14] M. I. Faley, Y. Liu, and R. E. Dunin-Borkowski, "Titanium nitride as a new prospective material for nanoSQUIDS and superconducting nanobridge electronics," *Nanomaterials*, vol. 11, 2021, Art. no. 466, doi: [10.1088/1361-6668/ac64cd](https://doi.org/10.1088/1361-6668/ac64cd).
- [15] M. I. Faley, T. Bikulov, V. Bosboom, A. A. Golubov, and R. E. Dunin-Borkowski, "Bulk nanomachining of cantilevers with Nb nanoSQUIDS based on nanobridge Josephson junctions," *Supercond. Sci. Technol.*, vol. 34, 2021, Art. no. 035014, doi: [10.1088/1361-6668/abda5c](https://doi.org/10.1088/1361-6668/abda5c).
- [16] B. Sauer, R. Gottfried-Gottfried, T. Haase, and H. Kück, "CMOS-compatible integration of thin ferromagnetic films," *Sensors Actuators A: Phys.*, vol. 42, no. 1/3, pp. 582–584, Apr. 1994, doi: [10.1016/0924-4247\(94\)80058-8](https://doi.org/10.1016/0924-4247(94)80058-8).
- [17] J. Williams, M. I. Faley, J. V. Vas, P. Lu, and R. E. Dunin-Borkowski, "TEM sample preparation of lithographically patterned permalloy nanostructures on silicon nitride membrane," *Beilstein J. Nanotechnol.*, vol. 15, pp. 1–12, 2024, doi: [10.3762/bjnano.15.1](https://doi.org/10.3762/bjnano.15.1).